

# Kinetics of Inhibition by Tyrphostins of the Tyrosine Kinase Activity of the Epidermal Growth Factor Receptor and Analysis by a New Computer Program

ISRAEL POSNER,<sup>1</sup> MICHAEL ENGEL, AVIV GAZIT, and ALEXANDER LEVITZKI

Department of Biological Chemistry (I.P., A.G., A.L.) and The Computation Center (M.E.), The Hebrew University of Jerusalem, Jerusalem, 91904, Israel

Received June 28, 1993; Accepted December 21, 1993

## SUMMARY

The kinetics of inhibition of the epidermal growth factor (EGF) receptor (EGFR) tyrosine kinase (TK) activity by erbstatin, tyrphostins, and lavendustin derivatives were studied in a system that employs poly(Glu<sub>6</sub>Ala<sub>3</sub>Tyr) (GAT) and ATP as substrates, after preactivation with EGF. All data were analyzed for computer best-fit curves by a program that was written for this purpose and is available upon request to those interested. The inhibition kinetics followed a sequential, Bi-Bi, rapid equilibrium, random mechanism, the mechanism of the EGFR-TK. Erbstatin and a few tyrphostins that contain a 3,4-dihydroxy-(*cis*)-cinnamionitrile [1-(3',4'-dihydroxyphenyl)-2-nitroethene] group were found to be pure competitive inhibitors with respect to both substrates of

the kinase reaction, i.e., GAT and ATP. Two tyrphostins, each containing an additional dihydroxyphenyl group in the  $\alpha$ -position, were found to be pure competitive inhibitors with respect to GAT and noncompetitive (or mixed-competitive) inhibitors with respect to ATP. A lavendustin derivative with a 2,5-dihydroxyphenyl ring and a lavendustin derivative with a 3,4-dihydroxyphenyl ring were also found to be competitive inhibitors with respect to both ATP and GAT. Various possible modes of binding at the EGFR-TK active center for the tyrphostins studied are proposed and the significance of the present findings, as well as the interpretation of computer analyses of kinetic data, is discussed.

The EGFR, like many proto-oncogene products, belongs to a growing family of PTKs that play an important role in signal transduction (1, 2). The activity of the TK domain, which is similar to that of many other oncogene products (3), is controlled by EGF and apparently plays a major role in the regulation of cell proliferation. EGFR undergoes autophosphorylation on tyrosine residues localized to the carboxyl terminus of the receptor and also phosphorylates external substrates. These two processes are markedly enhanced by EGF both *in vivo* and *in vitro*. Based on extensive and detailed kinetic studies with EGFR isolated from A431 cells, with GAT, angiotensin II, and ATP as substrates, we have recently concluded that the TK reaction follows a sequential, rapid equilibrium, random Bi-Bi mechanism (4).

In the past few years, our laboratory has embarked on the development of a series of TK inhibitors that have been termed

"tyrphostins" (5-9). We have shown that tyrphostins block EGF-dependent autophosphorylation, EGF-dependent phosphorylation of exogenous substrates (5-7), EGF-dependent cell proliferation (5, 10), EGF-dependent phosphorylation of phospholipase C- $\gamma$  (11), EGF-dependent breakdown of phosphoinositides by phospholipase C- $\gamma$  (12), and EGF-dependent proliferation of keratinocytes (13). While evaluating the effectiveness of newly synthesized tyrphostins as TK inhibitors, we were struck by the fact that small chemical modifications in the structures of tyrphostins have led to marked changes in their ability (a) to inhibit the TK activity of the EGFR and other TKs and (b) to distinguish between TKs, i.e., to selectively and effectively inhibit a given TK in comparison with another (5-7, 14, 15). We have, therefore, chosen to study the kinetic behavior of a group of tyrphostins representing four families of PTK blockers, with the intention of possibly gaining insights into the architecture of the active site. These studies were not designed to offer new insights into the function of the EGFR. For the purpose of comparison, we have included erbstatin, a natural product of *Streptomyces* sp. first isolated by Umezawa *et al.* (16), and two derivatives of lavendustin-A, a

This work was supported by grants from Rhône Poulenc Rorer (King of Prussia, PA), SUGEN, Inc. (Redwood City, CA), Misrad Haklita-Ministry of the Interior, and The Israel Cancer Association, through a contribution of Teva Pharmaceutical Industries, Ltd. (Jerusalem, Israel).

<sup>1</sup>I. P. is professor emeritus of Instituto de Medicina Experimental, Facultad de Medicina, Universidad Central de Venezuela, Caracas, Venezuela.

**ABBREVIATIONS:** EGFR, epidermal growth factor receptor; BMN, benzenemalononitrile; DMSO, dimethylsulfoxide; EGF, epidermal growth factor; GAT, poly(Glu<sub>6</sub>Ala<sub>3</sub>Tyr); MES, 2-(morpholino)ethanesulfonic acid; MLD, mean logarithmic deviation; PTK, protein tyrosine kinase catalytic subunit; TK, tyrosine kinase; EtAc, ethyl acetate; Ac, acetate; MS, mass spectrometry.

TK inhibitor isolated from *Streptomyces griseolavendus* by Onoda et al. (17), synthesized in our laboratory. We demonstrate that erbstatin, two lavendustin derivatives, and most of the tyrphostins studied interact with the active center of the EGFR and, in doing so, block the binding of both substrates of the kinase reaction. Two of the tyrphostins studied are competitive inhibitors with respect to GAT and noncompetitive inhibitors with respect to ATP. All experimental data were analyzed by a computer program written for the purpose of objectively analyzing enzyme kinetic data (4).

## Experimental Procedures

### Materials

Mouse EGF (tissue culture grade) was obtained from Serotec (Oxford, UK) and [ $\gamma$ - $^{32}$ P]ATP was purchased from Amersham Corp. (UK). GAT (M, 28,000) and ATP were purchased from Sigma Chemical Co. (St. Louis, MO). Agarose-immobilized wheat germ agglutinin was obtained from Biomakor (Rehovot, Israel). All other biochemicals were obtained from Sigma and were of the highest purity available; water was deionized by using a Barnsted Nanopure system.

### Tyrphostins

The tyrphostins used in these studies were synthesized as described elsewhere (6, 7). Here and also in other publications tyrphostins are catalogued according to the AG numbering. The RG numbers, when available, are in accord with the numbering system of Rhône Poulenc Rorer. The procedures for the synthesis of the new unreported tyrphostins were as follows.

**AG 799 (5-benzylthiomethylvanilline).** To 0.85 g (4.2 mM) of 5-CH<sub>2</sub>Cl-vanillin (18) and 0.5 ml of 4 mM benzylmercaptane in 30 ml of CH<sub>2</sub>Cl<sub>2</sub> was added 0.6 ml, 6 mM triethylamine. After stirring for 4 hr at room temperature, the reaction mixture was directly chromatographed to give white solid [0.45 g; 37% yield; m.p. 48°; NMR (CDCl<sub>3</sub>):  $\delta$  9.79 (1 H, s, CHO), 7.33 (7 H, br s), 3.96 (3 H, s, OCH<sub>3</sub>), 3.73 (2 H, s), and 3.71 (2 H, s) (16)].

**AG 800 [3-methoxy-4-hydroxy-5-benzylthiomethyl- $\alpha$ -amido-(*cis*)-cinnamitrile].** AG 799 (0.4 g, 14 mM) and 0.12 g (1.4 mM) of cyanoacetamide in 5 ml of ethanol, with three drops of piperidine, were refluxed for 1.5 hr. Water and HCl were added and the reaction mixture was extracted with EtAc. Evaporation gave 0.25 g (50% yield) of yellow solid [m.p. 150°; MS:  $m/z$  354 (M<sup>+</sup>, 29%), 232 (M-SCH<sub>2</sub>C<sub>6</sub>H<sub>5</sub>, 100%), 231 (42%), and 230 (52%); NMR (acetone-*d*<sub>6</sub>):  $\delta$  8.13 (1 H, s, vinyl), 7.71 (1 H, d,  $J$  = 2.0 Hz, H<sub>2</sub>), 7.58 (1 H, d,  $J$  = 2 Hz, H<sub>6</sub>), 7.40–7.25 (5 H, m), 3.94 (3 H, s, OCH<sub>3</sub>), 3.78 (2 H, s), and 3.75 (2 H, s)].

**AG 805 [ $\alpha$ -(3,4-dihydroxybenzoyl)-5-(*cis*)-indole-cinnamitrile].** 5-Formyl indole (130 mg, 1 mM), 180 mg (1 mM) of 2-cyano-3',4'-dihydroxyacetophenone (7), and 30 mg of  $\beta$ -alanine were refluxed for 3 hr, water was added, and the reaction mixture was extracted with EtAc to give an oily solid, containing some aldehyde. Chromatography gave a pure orange solid [86 mg; 28% yield; m.p. 185°; MS:  $m/z$  304 (M<sup>+</sup>, 8%), 177 (29%), 137 [C<sub>6</sub>H<sub>5</sub>(OH)<sub>2</sub>CO<sup>+</sup>, 100%], 117 (12%), 116 (indole<sup>+</sup>, 15%), and 109 (93%); NMR (acetone-*d*<sub>6</sub>):  $\delta$  8.40 (1 H, d,  $J$  = 1.6 Hz, H<sub>4</sub>), 8.18 (1 H, s, vinyl), 8.03 (1 H, dd,  $J$  = 8.6 and 1.6 Hz, H<sub>6</sub>), 7.63 (1 H, d,  $J$  = 8.6 Hz, H<sub>5</sub>), 7.54–7.40 (3 H, m, H<sub>3</sub> + H<sub>2,s</sub>), 7.0 (1 H, d,  $J$  = 8.6 Hz, H<sub>7</sub>), and 6.69 (1 H, d,  $J$  = 3.2 Hz, H<sub>2</sub>)].

**AG 814 [(2',5'-dihydroxy)benzyl-3-aminobenzoic acid].** *m*-Aminobenzoic acid (0.41 g, 3 mM) and 0.41 g (3 mM) of 2,5-dihydroxybenzaldehyde in 20 ml of CH<sub>3</sub>OH were refluxed for 16 hr (a red precipitate was formed). The reaction mixture was cooled to room temperature and 0.22 g (3.5 mM) of NaCNBH<sub>4</sub> was added. After stirring at room temperature for 2 hr, the reaction mixture was extracted with EtAc to give a yellow oil, which was triturated with CHCl<sub>3</sub> and filtered to give 0.2 g (26% yield) of a yellow solid [m.p. 145°; MS:  $m/z$  259 (M<sup>+</sup>, 9%), 241 (M-H<sub>2</sub>O, 21%), 137 (M-H-C<sub>6</sub>H<sub>4</sub>COOH, 100%), and 120 (54%); NMR (acetone-*d*<sub>6</sub>):  $\delta$  7.34–6.50 (7 H, m) and 4.34 (2 H, s).

**AG 824 [3,4-dihydroxy-5-benzylthiomethyl- $\alpha$ -amido-(*cis*)-cinnamitrile].** To 100 mg of 0.3 mM AG 800 in 20 ml of CH<sub>2</sub>Cl<sub>2</sub>, under argon, was added 0.6 ml of 6 mM BBr<sub>3</sub>. The orange solution was stirred for 2.5 hr at room temperature, water and HCl were added, and the reaction mixture was extracted with EtAc. Evaporation and trituration with EtAc/C<sub>6</sub>H<sub>6</sub> gave a dark yellow solid [40 mg; 42% yield; m.p. 190°; NMR (acetone-*d*<sub>6</sub>):  $\delta$  8.02 (1 H, s, vinyl), 7.63 (1 H, d,  $J$  = 2.2 Hz, H<sub>2</sub>), 7.38–7.20 (6 H, m), 3.77 (2 H, s), and 3.73 (2 H, s)].

**AG 826 [(3',4'-dihydroxy)benzyl-3-aminobenzoic acid].** 3,4-Dihydroxybenzaldehyde (0.41 g, 3 mM) and 0.41 g (3 mM) of *m*-aminobenzoic acid in 30 ml of methanol were refluxed for 16 hr and cooled, and 0.9 g of NaCNBH<sub>4</sub> was added. After 3 hr at room temperature, water was added and the reaction mixture was extracted with EtAc to give a yellow oil. Trituration with EtAc/CH<sub>2</sub>Cl<sub>2</sub> gave 20 mg of a yellow solid [2.5% yield; m.p. 140°; NMR (acetone-*d*<sub>6</sub>):  $\delta$  7.34–6.50 (7 H, m) and 4.22 (2 H, s)].

Tyrphostins were dissolved in DMSO immediately before each experiment and were diluted 10-fold with ethanol/H<sub>2</sub>O (1:1, v/v). Further dilutions were performed with DMSO/ethanol/H<sub>2</sub>O (1:4.5:4.5, v/v/v). This protocol ensured the complete solubility of all tyrphostins.

### Preparation of EGFR

EGFR was purified from human epidermoid carcinoma A431 cells as described elsewhere (4, 19) and was stored at -70°. When subjected to immunoblotting with an anti-EGFR antibody (monoclonal antibody 108, a gift from Dr. J. Schlessinger, New York University Medical School, and Dr. A. Zilberstein, Rhône Poulenc Rorer), the purified receptor appeared as one band (170 kDa) (data not shown). Also, when the receptor was subjected to treatment with ATP and EGF and then to immunoblotting using antiphosphotyrosine antibodies, a single 170-kDa band was observed.

### Assay of EGFR-TK Activity

Assays were performed in nonsterile culture plates with 96 conical wells (4, 20). Assay mixtures contained [ $\gamma$ - $^{32}$ P]ATP (2–3  $\mu$ Ci), fixed concentrations of GAT and increasing concentrations of ATP, or vice versa, 50 mM Tris-MES, and 60 mM MgAc<sub>2</sub>, pH 8.0, in total volumes of 20 ml plus 5.0  $\mu$ l of DMSO/ethanol/water or different fixed concentrations of tyrphostins dissolved in the same solvent system. Final DMSO and ethanol concentrations in the assay medium were 1.25% and 5.6%, respectively, and were found to reduce the maximal specific activity by <15%, compared with samples containing 50 mM Tris-MES buffer without solvents. EGFR was preactivated by incubation with EGF for 20 min at 4° immediately before use. Reactions were initiated by the simultaneous addition of activated EGFR to series of eight wells, with the aid of a multipipettor (15  $\mu$ l/well), after temperature equilibration of the EGFR preparations and the incubation medium to 22° for 2 min. After 4 min of incubation at 22°, 20-ml aliquots were transferred, with the aid of the multipipettor, from series of eight wells to eight corresponding Whatman no. 3MM paper strips (0.8  $\times$  30 mm) held in a 3-inch paper clamp. The paper strips were immediately released into a beaker containing 10% trichloroacetic acid and, after three 30-min washes and one overnight wash with 10% trichloroacetic acid, the strips were washed in ethanol and then in acetone and were dried. Radioactivity remaining on the filter strips was determined by Cerenkov counting in a Packard CD1600 scintillation counter. In each experiment appropriate blanks were run to correct for autophosphorylation and for nonspecific  $^{32}$ P labeling, and initial reaction velocities were expressed in terms of the rate of net phosphorylation of GAT. It should be mentioned that (a) autophosphorylation amounted to a small fraction of total TK activity, (b) reaction rates were linear over the 4-min period of incubation of EGFR and its substrates, (c) reaction rates were directly proportional to EGFR protein concentrations, and (d) in no case was >0.75% of any substrate consumed during the reaction.

### Determination of IC<sub>50</sub>

To determine computerized IC<sub>50</sub> values for different tyrphostins, the EGFR-TK activity were assayed at eight different tyrphostin

concentrations as described above, except that each assay system contained 125  $\mu\text{M}$  GAT (3 times its  $K_m$ ) and 125  $\mu\text{M}$  ATP (3.13 times its  $K_m$ ).

### Data Analysis

In kinetic studies, data are processed by one of a number of ways. Double-reciprocal plots are sometimes drawn by hand to fit the experimental data, thus introducing an obvious element of subjectivity into the interpretation of the experimental results. More often, velocity curves obtained at each fixed concentration of second substrate or inhibitor are individually subjected to computer analysis and double-reciprocal plots that are derived by linear or nonlinear regression analysis are then drawn as produced by the computer. Such curves seldom intersect at a single point; they often intersect one another at a number of points, a fact that is most compromising in experiments with only three or four double-reciprocal plots because it is almost impossible in such cases to determine the model followed by the reaction under study or to determine whether an inhibitor is competitive, noncompetitive, etc. If curves computed individually are hand-adjusted to intersect at a common point, an element of subjectivity is introduced into the interpretation of the experimental results. To overcome the aforementioned limitations and to avoid the need to rely on visual inspections of double-reciprocal plots as criteria for discriminating between kinetic models, all data in a previous work (4) were treated by a computer program that simultaneously analyzes all of the experimental points and fits them into the proper kinetic model. In the present work we have used this method to analyze 13 tyrrhostins, which represent four families of inhibitors (Table 1).

### Kinetic Analysis

Experiments were performed in duplicate and data were analyzed on the digital's visual memory system computer system by using a program written especially for this purpose (4), making use of the IMSL routine BCPOL (20a). This program is available upon request to all those interested. The procedure involves two steps. First, data analysis is aimed at determining  $K_A$ ,  $K_B$ ,  $V_{\max}$ , and  $\alpha$  in the nomenclature of Segel (21), which are equivalent to  $K_{i0}$ ,  $K_{s0}$ , the  $K_i/K_{i0}$  ratio, and the  $K_s/K_{s0}$  ratio, respectively, in the nomenclature of Cleland (21, 22), by fitting experimental data into eqs. 1 and 2 (Table 2). Next, all of the experimental  $v$  values that are a function of  $[A]$ ,  $[B]$ , and  $[I]$  are analyzed to extract optimal values of other parameters of interest, using the values of the constants obtained in the previous step. Theoretically, when this procedure is used, equations that yield best-fit curves, i.e., lowest MLD, express the proper model for the study in question. All plots shown in Results are computer-derived "best-fit" curves.

Equations 3 and 4 shown in Table 2 have been derived from model I shown below for "nonexclusive" or "partial" inhibition (21).

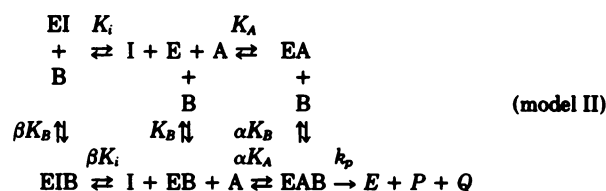
The above model invokes the formation of an active EIAB complex, which means that the inhibitor under consideration does not bind to either substrate A or substrate B binding sites on the enzyme. The Lineweaver-Burk plots for A or B as variables should intersect at points where:

$$\frac{1}{[A]} = \frac{(\delta - 1) + \frac{\alpha K_B}{[B]} (\delta - \beta)}{\alpha K_A [(\gamma - \delta) + \frac{K_B}{[B]} (\beta\gamma - \delta)]} \quad (3i)$$

and

$$\frac{1}{[B]} = \frac{(\delta - 1) + \frac{\alpha K_A}{[A]} (\delta - \gamma)}{\alpha K_B [(\beta - \delta) + \frac{K_A}{[A]} (\beta\gamma - \delta)]} \quad (4i)$$

In Table 2, eq. 5, which expresses the kinetics of inhibitors competitive with substrate A, and eq. 8, which expresses the kinetics of inhibitors noncompetitive (or mixed-competitive) with substrate B, were derived from the following model for dead-end EIB (21):



When substrate B is varied at constant  $[A]$ , the double-reciprocal plots should intersect at a point equal to  $-1/\beta K_i$ . A similar model with dead-end EIA for inhibitors competitive with substrate B and noncompetitive (or mixed-competitive) with substrate A is expressed by eqs. 6 and 7, respectively. In these equations  $\gamma K_A$  and  $\gamma K_i$  are the dissociation constants for the breakdown of EIA to  $A + \text{EI}$  or  $\text{I} + \text{EA}$ , respectively. When substrate A is varied at constant  $[B]$ , the double-reciprocal plots should intersect at a point equal to  $-1/\gamma K_i$ .

Equations 9 and 10 in Table 2, which express the inhibition kinetics for compounds that are competitive inhibitors with respect to both substrates, express the following model (23):

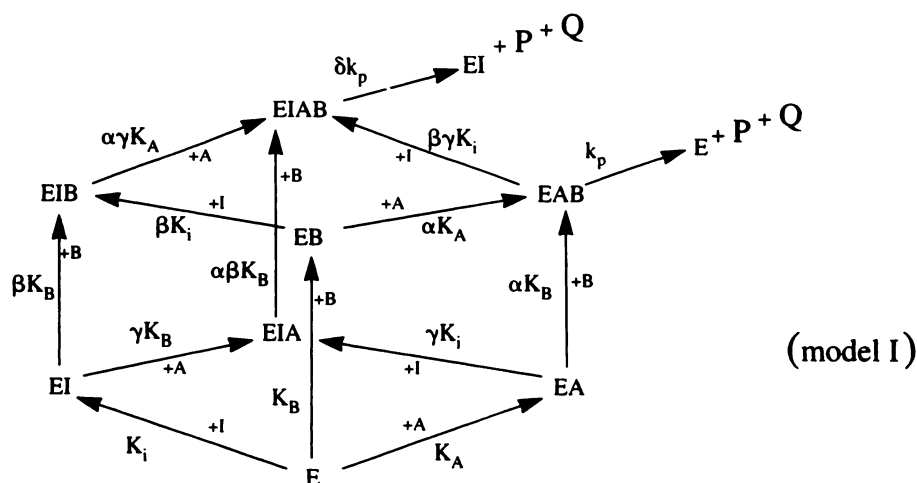
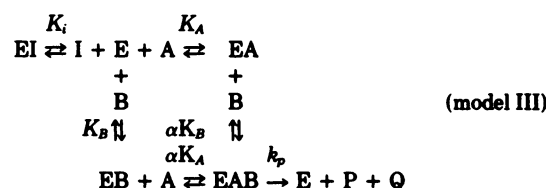
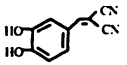
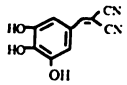
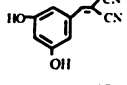
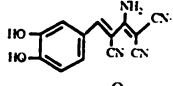
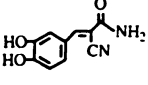
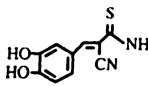
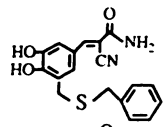
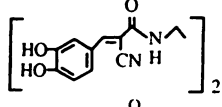
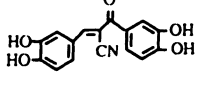
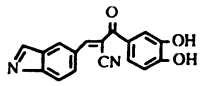
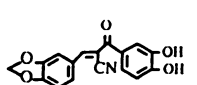
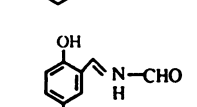
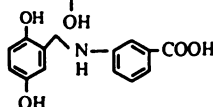
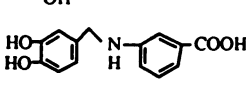




TABLE 1

Chemical structures, IC<sub>50</sub> values, and K<sub>i</sub> values of inhibitors of EGFR-TK activity

Inhibitor	Structure	IC <sub>50</sub> μM	K <sub>i</sub> μM
AG 18		10.0	7.4
AG 82		3.0	1.5
AG 83		37.0	16.5
AG 114		2.4	1.3
AG 99		9.4	2.3
AG 213		2.3	1.2
AG 824		1.0	0.6
AG 537		0.4	0.24
AG 538		0.4	0.18
AG 805		1.2	0.6
AG 468		9.2	1.6
Erbstatin		2.0	0.25
AG 814		0.6	0.4
AG 826		2.7	1.3

It should be pointed out that our program, like any other computer program, aims at fitting experimental data to an equation that expresses a given theoretical model. In doing so, the program assigns and reassigns values to kinetic constants that appear in the equation until the lowest possible MLD value is reached, i.e., best fit is attained. Consequently, the MLD value alone is not always a sufficient criterion for discriminating between models. This important attribute of the computer analysis of kinetic data is neither a limitation nor a drawback and can be readily understood once it is realized that the computer can convert an equation that expresses an "ill-fitted" model to an equation

TABLE 2

Mathematical expressions of the various kinetic models discussed in Data Analysis

(i) Sequential Bi-Bi rapid equilibrium random mechanism for variable [A]

$$\frac{1}{v_{cal}} = \frac{1}{v_{max}} \left[ \left( 1 + \frac{K_B}{[B]} \right) \frac{\alpha K_A}{[A]} + \left( 1 + \frac{\alpha K_B}{[B]} \right) \right] \quad (1)$$

or, if [B] is variable

$$\frac{1}{v_{cal}} = \frac{1}{v_{max}} \left[ \left( 1 + \frac{K_A}{[A]} \right) \frac{\alpha K_B}{[B]} + \left( 1 + \frac{\alpha K_A}{[A]} \right) \right] \quad (2)$$

(ii) Partial or nonexclusive inhibition mechanism

$$\frac{1}{v_{cal}} = \frac{\left( 1 + \frac{K_B}{[B]} + \frac{[I]}{\beta K_i} + \frac{K_B[I]}{[B]K_i} \right) \frac{\alpha K_A}{[A]} + \left( 1 + \frac{\alpha K_B}{[B]} + \frac{[I]}{\beta \gamma K_i} + \frac{\alpha K_B[I]}{\gamma [B]K_i} \right)}{v_{max} \left( 1 + \frac{\delta [I]}{\beta \gamma K_i} \right)} \quad (3)$$

or

$$\frac{1}{v_{cal}} = \frac{\left( 1 + \frac{K_A}{[A]} + \frac{[I]}{\gamma K_i} + \frac{K_A[I]}{[A]K_i} \right) \frac{\alpha K_B}{[B]} + \left( 1 + \frac{\alpha K_A}{[A]} + \frac{[I]}{\beta \gamma K_i} + \frac{\alpha K_A[I]}{\beta [A]K_i} \right)}{v_{max} \left( 1 + \frac{\delta [I]}{\beta \gamma K_i} \right)} \quad (4)$$

(iii) Competitive inhibition mechanism

$$\frac{1}{v_{cal}} = \frac{\left( 1 + \frac{K_B}{[B]} + \frac{[I]}{\beta K_i} + \frac{K_B[I]}{[B]K_i} \right) \frac{\alpha K_A}{[A]} + \left( 1 + \frac{\alpha K_B}{[B]} \right)}{v_{max}} \quad (5)$$

or

$$\frac{1}{v_{cal}} = \frac{\left( 1 + \frac{K_A}{[A]} + \frac{[I]}{\gamma K_i} + \frac{K_A[I]}{[A]K_i} \right) \frac{\alpha K_B}{[B]} + \left( 1 + \frac{\alpha K_A}{[A]} \right)}{v_{max}} \quad (6)$$

(iv) Noncompetitive inhibition mechanism

$$\frac{1}{v_{cal}} = \frac{\left( 1 + \frac{K_B}{[B]} + \frac{K_B[I]}{[B]K_i} \right) \frac{\alpha K_A}{[A]} + \left( 1 + \frac{\alpha K_B}{[B]} + \frac{\alpha K_B[I]}{\gamma [B]K_i} \right)}{v_{max}} \quad (7)$$

or

$$\frac{1}{v_{cal}} = \frac{\left( 1 + \frac{K_A}{[A]} + \frac{K_A[I]}{[A]K_i} \right) \frac{\alpha K_B}{[B]} + \left( 1 + \frac{\alpha K_A}{[A]} + \frac{\alpha K_A[I]}{\beta [A]K_i} \right)}{v_{max}} \quad (8)$$

(v) Inhibition competitive with both substrates mechanism

$$\frac{1}{v_{cal}} = \frac{1}{v_{max}} \left[ \left( 1 + \frac{K_B}{[B]} \left( 1 + \frac{[I]}{K_i} \right) \right) \frac{\alpha K_A}{[A]} + \left( 1 + \frac{\alpha K_B}{[B]} \right) \right] \quad (9)$$

$$\frac{1}{v_{cal}} = \frac{1}{v_{max}} \left[ \left( 1 + \frac{K_A}{[A]} \left( 1 + \frac{[I]}{K_i} \right) \right) \frac{\alpha K_B}{[B]} + \left( 1 + \frac{\alpha K_A}{[A]} \right) \right] \quad (10)$$

that expresses the best-fit model simply by properly adjusting the values of kinetic parameters. This point and the correct handling and interpretation of computer output information are illustrated below for various models. (a) The correct model is the partial-inhibition model (model I); in this case the MLD values would likely be sufficient for distinguishing between different models, and secondary plots are hyperbolic. (b) The correct model is the noncompetitive inhibition model; in this case similar MLD values may be obtained while fitting the data

into eqs. 3 and 4, expressing the partial inhibition model, or into eqs. 7 or 8, expressing the noncompetitive inhibition model. However, a careful analysis of the computer output would reveal that for eqs. 3 and 4 large values have been assigned to  $\beta$  or  $\gamma$ , irrespective of whether or not  $\delta$  is small, such that EIAB and either EIA or EIB complexes seen in model I cannot form. Because for large  $\beta$  in eq. 3 the ratios  $\delta[I]/\beta\gamma K_i$ ,  $[I]/\beta\gamma K_i$ , and  $[I]/\beta K_i$  cancel out, this equation is reduced in reality to eq. 7. Similarly, for large  $\gamma$  in eq. 4 the ratios  $\delta[I]/\beta\gamma K_i$ ,  $[I]/\beta\gamma K_i$ , and  $[I]/\gamma K_i$  cancel out and this equation is reduced to eq. 8. In other words, the best fit is indeed that obtained for noncompetitive inhibition. Secondary plots, of course, are identical and linear in both cases. It may be noted that eqs. 5 and 6, expressing competitive inhibition, can in no way be converted to those expressing either noncompetitive or partial-competitive inhibition. Consequently, fitting the experimental data into eqs. 5 or 6 yields much higher MLD values (poor fits) than does fitting into eqs. 7 and 8, respectively, i.e., the MLD values should be sufficient for discriminating between noncompetitive and competitive inhibition. (c) The correct model is the competitive inhibition model; it readily follows that, similarly to the situation described above, eqs. 3 and 4, expressing partial inhibition, can be reduced to expressions of competitive inhibition (eqs. 5 and 6, respectively) if  $\beta$  and  $\gamma$  are assigned large enough values, whether or not  $\delta$  is small. Equations 7 and 8 for noncompetitive inhibition can also be reduced to eqs. 5 and 6 for competitive inhibition if  $\beta$  or  $\gamma$ , respectively, are large. Hence, if similar MLD values are obtained for best fits of experimental data to partial-inhibition, noncompetitive inhibition, and competitive inhibition models, an analysis of the constants  $\beta$ ,  $\gamma$ , and  $\delta$ , as well as  $K_A$ ,  $K_B$ , and  $K_i$ , should follow to confirm the tendency of the computer program to reduce all equations to those expressing competitive inhibition as the correct model in question. This tendency should be considered as confirmatory of competitive inhibition.

## Results

In the present studies the overall MLD oscillated between 0.078 and 0.153. In other words, the overall experimental error was between 7 and 16%, values acceptable for experiments of this nature (24). The computed average  $K_{GAT}$  and  $K_{ATP}$  values were  $62.5 \pm 15.2 \mu\text{M}$  and  $44.5 \pm 12.7 \mu\text{M}$ , respectively, and  $\alpha$  was  $1.4 \pm 0.5$ , values similar to those obtained earlier (4).

### Effects of Various Tyrphostins on the PTK Activity of EGFR

The inhibition of EGFR-TK by a number of tyrphostins was examined and the  $IC_{50}$  values for each inhibitor were computed (Table 1). All of the tyrphostins studied, with the exception of AG 18 and AG 83, inhibited the EGFR-TK activity with  $IC_{50}$  values of  $<10.0 \mu\text{M}$ .

### Kinetics of EGFR-TK Activity

For each of the aforementioned tyrphostins and TK inhibitors, the kinase activities of EGFR preparations that had been preactivated at  $4^\circ$  with 900 nM EGF for 20 min were determined at six constant concentrations of the tyrphostin as a function of eight concentrations of GAT and a fixed concentration of ATP or as a function of eight concentrations of ATP and a fixed concentration of GAT, to ensure the accumulation of sufficient experimental data for the computer best-fit analysis. In each experiment,  $K_{GAT}$ ,  $K_{ATP}$ ,  $V_{max}$ , and  $\alpha$  values were first calculated from computer-fitted plots at zero tyrphostin concentrations (4), using eqs. 1 or 2 (Table 2). These values were then introduced into the various equations to obtain computer-fitted best-fit curves, from which the appropriate model for

each tyrphostin was ascertained and on the basis of which appropriate kinetic constants were computerized.

### Inhibitors that Compete with Both Substrates

Erbstatin, the lavendustin derivatives AG 814 and AG 826, the dicyano-tyrphostin derivatives AG 18, AG 82, and AG 83, AG 114 with a dicyanoaminoethylene group, and the dihydroxymalononitrile derivatives AG 99, AG 213 (RG 50864), and AG 824 all behaved as competitive inhibitors with respect to both GAT and ATP. The two tyrphostins AG 805 and AG 468, which contain only the second dihydroxyphenyl ring of AG 538 in the  $\alpha$ -position (Table 1), were also competitive inhibitors with respect to both GAT and ATP. For all of the aforementioned tyrphostins the proper kinetic model could not be assigned solely on the basis of differences between MLD values, i.e., MLD values obtained for "fits" into eqs. 3, 5, 7, and 9 with [ATP] as variable or into eqs. 4, 6, 8, and 10 with [GAT] as the varied substrate were either very similar or identical (data for representative compounds are shown in Table 3). Hence, values of the kinetic constants obtained in each fit were substituted into appropriate equations expressing the model being evaluated, as described in Data Analysis. It was found that, when this was done, these expressions always reduced to expressions of competitive inhibition. Computed double-reciprocal plots and slope replots, i.e., secondary plots, obtained by fitting the experimental data for a given inhibitor at constant GAT and variable ATP concentrations, or vice versa, to four different models were identical or very similar. This is illustrated in Figs. 1-4 for a representative case of the TK inhibitor erbstatin.

### Inhibitors that Compete Only with the Peptide Substrate

AG 537. Based of the results of computer analysis of kinetic data of experiments with AG 537, which is a "dimer" of AG 99 (Table 1), it has been concluded that this compound is a competitive inhibitor with respect to GAT and a noncompetitive inhibitor with respect to ATP. It should be noted that, in the case of GAT as the independent variable, the MLD values for fits to eqs. 4, 6, 8, and 10 are not significantly different. According to the rationale presented in Data Analysis, this is consistent with competitive inhibition. For fits to eq. 4,  $\beta$  and  $\gamma$  values of 4.4 and 18.1, respectively, were computed (Table 3). Thus, for example, at a constant [ATP] equal to  $K_{ATP}$  and a [I] equal to  $K_i$ , the y-intercept equals  $2.058/V_{max}$  instead of  $2.000/V_{max}$ . In other words, [I] has a negligible effect on  $V_{max}$ , but it still affects the slope, consistent with competitive inhibition. For fits to eq. 8 (Table 3), the y-intercept equals  $2.22/V_{max}$  instead of  $2.00/V_{max}$ . Again [I] is found to have a relatively small effect on  $V_{max}$ . On the other hand, with ATP as the independent variable the MLD values for fits to eq. 7, which expresses the model for noncompetitive inhibition, are considerably lower than the MLD values computed for fits to eq. 5, which expresses competitive inhibition kinetics. The differences between the MLD values for fits to eqs. 3 and 7 are not as large, but they are definitely in favor of the latter. Moreover, because AG 537 is a competitive inhibitor with respect to GAT, it can only be noncompetitive with respect to ATP. Thus, the kinetic studies with GAT and ATP as independent substrates complement each other. The double-reciprocal plots for a representative experiment with AG 537 as inhibitor are shown in Fig. 5, in which ATP was the varied substrate, and Fig. 7, in which GAT was the varied substrate. It can be readily seen that Fig. 5C represents a far better fit than Fig. 5, B or D.

TABLE 3

Values of kinetic constants computed from experimental data obtained with representative EGFR-TK inhibitors listed in Table 1 by fitting to different kinetic models

Values are means  $\pm$  standard deviations of two or three experiments.

Equation	Kinetic constants					MLD
	$\alpha^a$	$\beta^b$	$\gamma^c$	$\delta^d$	$K_i$	
						$\mu\text{M}$
<b>AG 537</b>						
3 <sup>e</sup>	1.2 $\pm$ 0.3	5.0 $\pm$ 1.4	1.9 $\pm$ 0.5	0.016 $\pm$ 0.018	0.38 $\pm$ 0.11	0.091 $\pm$ 0.015
5 <sup>e</sup>	1.2 $\pm$ 0.3	6.8 $\pm$ 7.6			0.44 $\pm$ 0.37	0.123 $\pm$ 0.007
7 <sup>e</sup>	1.2 $\pm$ 0.3		2.1 $\pm$ 0.8		0.24 $\pm$ 0.02	0.087 $\pm$ 0.016
9 <sup>e</sup>	1.2 $\pm$ 0.3				0.16 $\pm$ 0.06	0.128 $\pm$ 0.016
4 <sup>f</sup>	1.3 $\pm$ 0.1	4.4 $\pm$ 0.9	18.1 $\pm$ 3.4	0.004 $\pm$ 0.001	0.13 $\pm$ 0.03	0.096 $\pm$ 0.003
6 <sup>f</sup>	1.3 $\pm$ 0.1		1.5 $\pm$ 0.5		0.23 $\pm$ 0.01	0.104 $\pm$ 0.015
8 <sup>f</sup>	1.3 $\pm$ 0.1	4.4 $\pm$ 0.5			0.12 $\pm$ 0.01	0.091 $\pm$ 0.002
10 <sup>f</sup>	1.3 $\pm$ 0.1				0.09 $\pm$ 0.01	0.099 $\pm$ 0.014
<b>AG 538</b>						
3 <sup>e</sup>	1.5 $\pm$ 0.6	3.5 $\pm$ 1.3	1.3 $\pm$ 2.4	0.001 $\pm$ 0.003	0.20 $\pm$ 0.02	0.098 $\pm$ 0.004
5 <sup>e</sup>	1.5 $\pm$ 0.6	43.2 $\pm$ 15.1			0.16 $\pm$ 0.01	0.152 $\pm$ 0.03
7 <sup>e</sup>	1.5 $\pm$ 0.6		1.8 $\pm$ 0.5		0.18 $\pm$ 0.05	0.088 $\pm$ 0.003
9 <sup>e</sup>	1.5 $\pm$ 0.6				0.11 $\pm$ 0.01	0.305 $\pm$ 0.037
4 <sup>f</sup>	1.7 $\pm$ 0.4	4.5 $\pm$ 1.4	13.2 $\pm$ 1.5	0.36 $\pm$ 0.07	0.13 $\pm$ 0.05	0.127 $\pm$ 0.022
6 <sup>f</sup>	1.7 $\pm$ 0.4		3.5 $\pm$ 0.7		0.16 $\pm$ 0.03	0.131 $\pm$ 0.018
8 <sup>f</sup>	1.7 $\pm$ 0.4	5.0 $\pm$ 1.8			0.12 $\pm$ 0.02	0.122 $\pm$ 0.020
10 <sup>f</sup>	1.7 $\pm$ 0.4				0.11 $\pm$ 0.01	0.125 $\pm$ 0.02
<b>Erbstatin</b>						
3 <sup>e</sup>	1.2 $\pm$ 0.2	22.6 $\pm$ 5.0	21.6 $\pm$ 15.0	11.4 $\pm$ 7.5	0.13 $\pm$ .05	0.147 $\pm$ 0.05
5 <sup>e</sup>	1.2 $\pm$ 0.2	21.4 $\pm$ 13.7			0.41 $\pm$ 0.17	0.187 $\pm$ 0.03
7 <sup>e</sup>	1.2 $\pm$ 0.2		603.0 $\pm$ 400		0.33 $\pm$ 0.14	0.186 $\pm$ 0.028
9 <sup>e</sup>	1.2 $\pm$ 0.2				0.22 $\pm$ 0.05	0.185 $\pm$ 0.025
4 <sup>f</sup>	1.5 $\pm$ 0.2	38.3 $\pm$ 33.6	9.3 $\pm$ 4.7	13.1 $\pm$ 15.4	0.28 $\pm$ 0.10	0.169 $\pm$ 0.017
6 <sup>f</sup>	1.5 $\pm$ 0.2		32.4 $\pm$ 30.0		0.32 $\pm$ 0.44	0.183 $\pm$ 0.011
8 <sup>f</sup>	1.5 $\pm$ 0.2	68.4 $\pm$ 80.0			0.134 $\pm$ 0.21	0.1800 $\pm$ 0.009
10 <sup>f</sup>	1.5 $\pm$ 0.2				0.11 $\pm$ 0.01	0.192 $\pm$ 0.034
<b>AG 213</b>						
3 <sup>e</sup>	1.0 $\pm$ 0.2	57 $\pm$ 13	12.4 $\pm$ 3.7	2.7 $\pm$ 1.8	1.7 $\pm$ 0.8	0.067 $\pm$ 0.004
5 <sup>e</sup>	1.0 $\pm$ 0.2	16.7 $\pm$ 14			2.2 $\pm$ 0.2	0.068 $\pm$ 0.005
7 <sup>e</sup>	1.0 $\pm$ 0.2		122 $\pm$ 38		1.7 $\pm$ 0.65	0.064 $\pm$ 0.002
9 <sup>e</sup>	1.0 $\pm$ 0.2				1.8 $\pm$ 0.9	0.069 $\pm$ 0.003
4 <sup>f</sup>	1.4 $\pm$ 0.6	45.3 $\pm$ 22.3	1.35 $\pm$ 0.15	0.155 $\pm$ 0.125	1.4 $\pm$ 0.5	0.174 $\pm$ 0.003
6 <sup>f</sup>	1.4 $\pm$ 0.6		86.5 $\pm$ 34.5		0.7 $\pm$ 0.2	0.181 $\pm$ 0.019
8 <sup>f</sup>	1.4 $\pm$ 0.6	261 $\pm$ 68			0.63 $\pm$ 0.17	0.170 $\pm$ 0.009
10 <sup>f</sup>	1.4 $\pm$ 0.6				0.51 $\pm$ 0.05	0.173 $\pm$ 0.019
<b>AG 805</b>						
3 <sup>e</sup>	1.1 $\pm$ 0.2	45.2 $\pm$ 16.5	3.4 $\pm$ 1.3	18 $\pm$ 5.9	0.2 $\pm$ 0.1	0.081 $\pm$ 0.013
5 <sup>e</sup>	1.1 $\pm$ 0.2	14.8 $\pm$ 3.6			0.8 $\pm$ 0.3	0.103 $\pm$ 0.014
7 <sup>e</sup>	1.1 $\pm$ 0.2		33 $\pm$ 14		0.7 $\pm$ 0.2	0.098 $\pm$ 0.013
9 <sup>e</sup>	1.1 $\pm$ 0.2				0.4 $\pm$ 0.2	0.1000 $\pm$ 0.014
4 <sup>f</sup>	1.5 $\pm$ 0.7	5.7 $\pm$ 3.9	10.4 $\pm$ 6.0	2.2 $\pm$ 1.4	0.3 $\pm$ 0.2	0.106 $\pm$ 0.015
6 <sup>f</sup>	1.5 $\pm$ 0.7		12.6 $\pm$ 1.4		0.7 $\pm$ 0.2	0.118 $\pm$ 0.016
8 <sup>f</sup>	1.5 $\pm$ 0.7	78 $\pm$ 9			0.6 $\pm$ 0.3	0.115 $\pm$ 0.017
10 <sup>f</sup>	1.5 $\pm$ 0.7				0.5 $\pm$ 0.1	0.116 $\pm$ 0.017
<b>AG 826</b>						
3 <sup>e</sup>	1.0 $\pm$ 0.1	332 $\pm$ 75	15.4 $\pm$ 9.4	1.54 $\pm$ 1.25	0.6 $\pm$ 0.3	0.116 $\pm$ 0.045
5 <sup>e</sup>	1.0 $\pm$ 0.1	14.8			1.43 $\pm$ 0.26	0.109 $\pm$ 0.044
7 <sup>e</sup>	1.0 $\pm$ 0.1		195 $\pm$ 48		0.8 $\pm$ 0.3	0.110 $\pm$ 0.044
9 <sup>e</sup>	1.0 $\pm$ 0.1				0.83 $\pm$ 0.24	0.105 $\pm$ 0.042
4 <sup>f</sup>	1.3 $\pm$ 0.5	230 $\pm$ 39	11.7 $\pm$ 1.6	6.4 $\pm$ 8.9	1.6 $\pm$ 0.9	0.145 $\pm$ 0.031
6 <sup>f</sup>	1.3 $\pm$ 0.5		10.8 $\pm$ 2.6		1.8 $\pm$ 0.5	0.142 $\pm$ 0.031
8 <sup>f</sup>	1.3 $\pm$ 0.5	74 $\pm$ 9			1.7 $\pm$ 0.4	0.139 $\pm$ 0.030
10 <sup>f</sup>	1.3 $\pm$ 0.5				1.3 $\pm$ 0.7	0.137 $\pm$ 0.030

<sup>a</sup>  $\alpha K_{\text{GAT}}$  and  $\alpha K_{\text{ATP}}$  are the constants for dissociation of E-GAT-ATP to E-GAT + ATP or E-ATP + GAT.

<sup>b</sup>  $\beta K_{\text{ATP}}$  and  $\beta K_i$  are the constants for dissociation of E-I-ATP to E-I + ATP or E-ATP + I.

<sup>c</sup>  $\gamma K_{\text{GAT}}$  and  $\gamma K_i$  are the constants for dissociation of E-I-GAT to E-I + GAT or E-GAT + I.

<sup>d</sup>  $\delta K_{\text{cat}}$  is the catalytic rate constant for the breakdown of E-I-GAT-ATP to E-I + P + Q.

<sup>e</sup> Variable ATP and constant GAT (80 or 400  $\mu\text{M}$ ).

<sup>f</sup> Variable GAT and constant ATP (40  $\mu\text{M}$  or 250  $\mu\text{M}$ ).

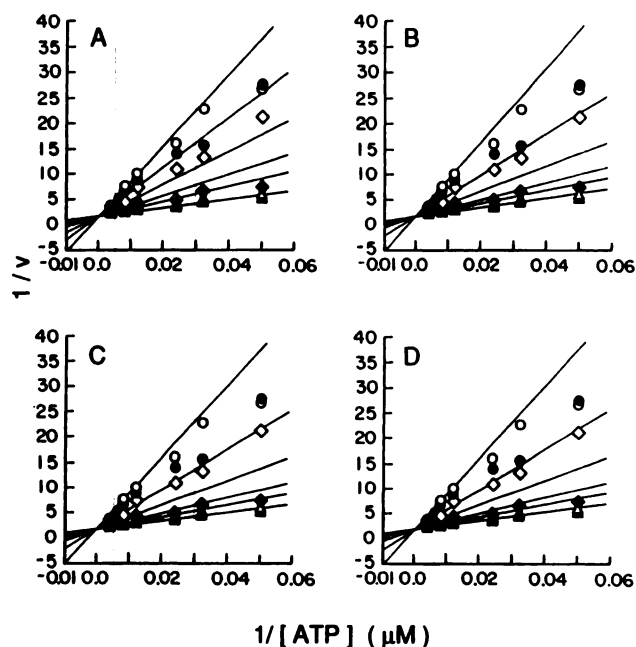


**Fig. 1.** Kinetics of inhibition of the EGFR-TK reaction by erbatatin. The activity of the EGFR was determined after a 20-min preactivation at 4° in the presence of EGF. Preactivated EGFR (15  $\mu$ l) was added to 25  $\mu$ l of medium containing varying concentrations of ATP, 60 mM  $\text{MgAc}_2$ , 50 mM Tris-MES, pH 7.6, 1.5–2.5  $\mu\text{Ci}$  of  $[\gamma\text{-}^{32}\text{P}]\text{ATP}$ , a fixed concentration of GAT (400  $\mu\text{M}$ ), and the following concentrations of erbatatin:  $\Delta$ , 0.0;  $\triangle$ , 0.37;  $\diamond$ , 0.74;  $\square$ , 1.58;  $\bullet$ , 3.16;  $\circ$ , 6.33  $\mu\text{M}$ . After 4 min at 22°, 20- $\mu$ l aliquots of each medium were transferred to Whatman 3MM filter paper strips, which were immediately dropped into 10% trichloroacetic acid. The strips were washed as described in Experimental Procedures and the radioactivity of phosphorylated GAT was determined by Cerenkov counting. Initial reaction velocity ( $v$ ) is expressed as [phosphorylated GAT] ( $\mu\text{M}$ )/assay system. The experimental results were analyzed as described in Data Analysis. Families of double-reciprocal plots for fits to eq. 3 for nonexclusive or partial inhibition (A), eq. 5 for competitive inhibition (B), eq. 7 for noncompetitive (or mixed-competitive) inhibition (C), or eq. 9 for inhibition competitive with both substrates (D) are shown.

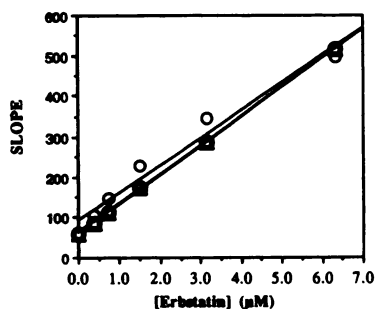


**Fig. 2.** Slope replots of the four families of double-reciprocal plots shown in Fig. 1, A ( $\circ$ ), B ( $\bullet$ ), C ( $\Delta$ ), and D ( $\square$ ).

Secondary plots computed for these experiments are shown in Figs. 6 and 8, respectively. It should be noted that the secondary plots shown in Fig. 6 for the family of double-reciprocal plots shown in Fig. 5, A and C, are both straight lines that overlap one another and both are distinctly different from the secondary plots in Fig. 6 for the double-reciprocal plots of Fig. 5, B and D. On the other hand, the four replots shown in Fig. 8 are very similar to one another.

**AG 538.** This tyrphostin yields kinetic data that fit best into a model for competitive inhibition with respect to GAT and noncompetitive inhibition with respect to ATP. This con-

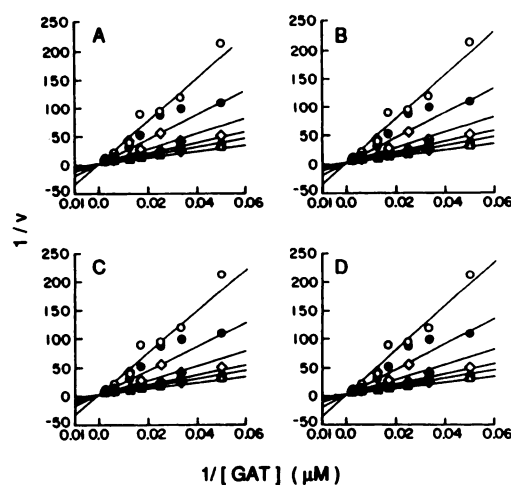


**Fig. 3.** Kinetics of inhibition of the EGFR-TK reaction by erbatatin. The activity of EGFR was determined as described in the legend to Fig. 1, except that medium contained varying concentrations of GAT, 60 mM  $\text{MgAc}_2$ , 50 mM Tris-MES, pH 7.6, 1.5–2.5  $\mu\text{Ci}$  of  $[\gamma\text{-}^{32}\text{P}]\text{ATP}$ , a fixed concentration of ATP (250  $\mu\text{M}$ ), and the following concentrations of erbatatin:  $\Delta$ , 0.00;  $\triangle$ , 0.37;  $\diamond$ , 0.74;  $\square$ , 1.58;  $\bullet$ , 3.16;  $\circ$ , 6.33  $\mu\text{M}$ . The experimental results were analyzed as described in Data Analysis. Families of double-reciprocal plots for fits to eq. 4 for nonexclusive or partial inhibition (A), eq. 6 for competitive inhibition (B), eq. 8 for noncompetitive (or mixed-competitive) inhibition (C), or eq. 10 for inhibition competitive with both substrates (D) are shown.

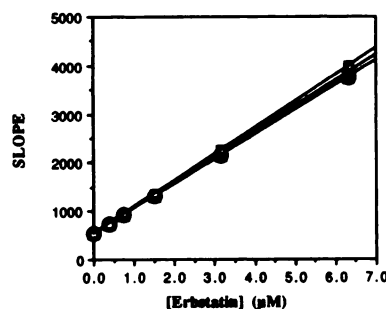


**Fig. 4.** Slope replots of the family of curves shown in Fig. 3, A ( $\circ$ ), B ( $\bullet$ ), C ( $\Delta$ ), and D ( $\square$ ).

clusion is based on the results of computer analysis of the data for inhibition experiments with AG 538 that are shown in Table 3, using the rationale presented in Data Analysis. For fits to eq. 4,  $\beta$  and  $\gamma$  values of 4.5 and 13.2, respectively, were computed (Table 3). Thus, for example, at a constant [ATP] equal to  $K_{\text{ATP}}$  and a [I] equal to  $K_i$ , the y-intercept equals  $2.094/V_{\text{max}}$  instead of  $2.000/V_{\text{max}}$ . For fits to eq. 8 (Table 3) the y-intercept equals  $2.20/V_{\text{max}}$  instead of  $2.00/V_{\text{max}}$ . Again [I] is found to have a relatively small effect on  $V_{\text{max}}$ . On the other hand, with ATP as the independent variable the MLD values for fits to eq. 7, which expresses the model for noncompetitive inhibition, are considerably lower than the MLD values computed for fits to eq. 5, which expresses competitive inhibition kinetics. The double-reciprocal plots for a representative experiment with AG 538 as inhibitor are shown in Fig. 9, in which ATP was the varied substrate, and Fig. 11, in which GAT was the varied substrate. It can be readily seen that Fig. 11C represents a far better fit than Fig. 11, B and D. Secondary plots computed for these experiments are shown in Figs. 10 and 12, respectively. It should be noted that the secondary plots shown in Fig. 10 for the family of double-reciprocal plots shown in Figs. 11, A and C, are both straight lines that overlap one



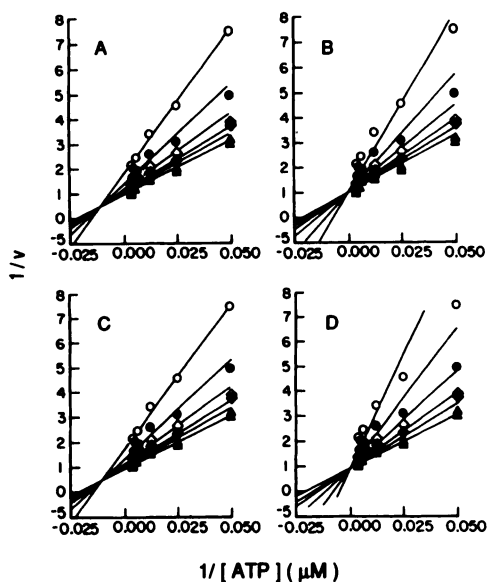


**Fig. 5.** Kinetics of inhibition of the EGFR-TK reaction by AG 537. The activity of EGFR was determined as described in the legend to Fig. 1 at the following concentrations of AG 537:  $\Delta$ , 0.0;  $\triangle$ , 0.13;  $\diamond$ , 0.25;  $\square$ , 0.50;  $\bullet$ , 1.00;  $\circ$ , 2.0  $\mu M$ . The experimental results were analyzed as described in Data Analysis. Families of double-reciprocal plots for fits to eq. 3 for nonexclusive or partial inhibition (A), eq. 5 for competitive inhibition (B), eq. 7 for noncompetitive (or mixed-competitive) inhibition (C), or eq. 9 for inhibition competitive with both substrates (D) are shown.

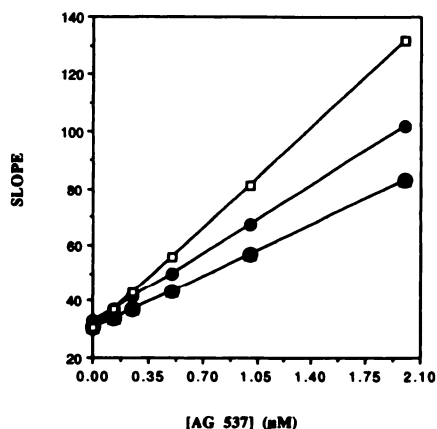
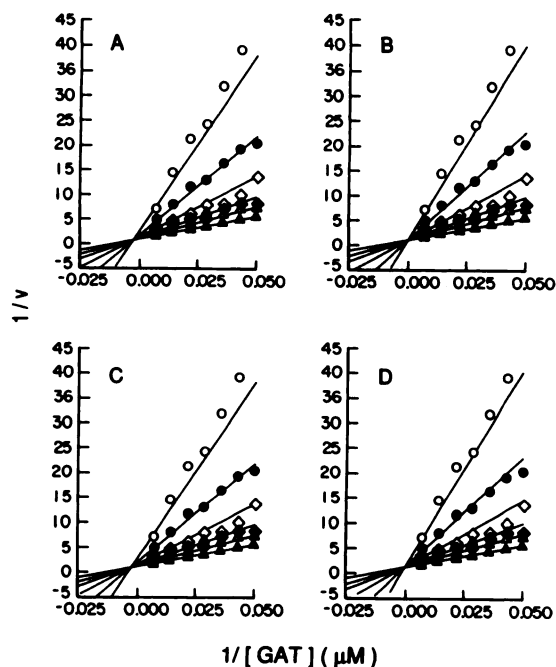


**Fig. 6.** Slope replots of the four families of double-reciprocal plots shown in Fig. 5, A ( $\circ$ ), B ( $\bullet$ ), C ( $\Delta$ ), and D ( $\square$ ).

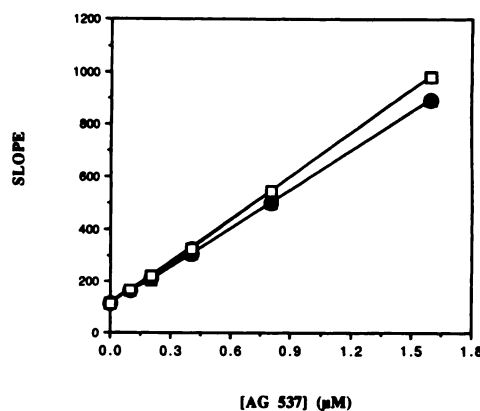
another and both are distinctly different from the secondary plots in Fig. 6 for the double-reciprocal plots of Fig. 11, B and D. On the other hand, the four replots shown in Fig. 12 are very similar to one another. Thus, the overall trends of the primary and secondary plots for this inhibitor were very similar to those shown for AG 537.

## Discussion

We have shown recently that the EGFR-TK reaction in our system follows a sequential, rapid equilibrium, Bi-Bi random mechanism (4). It is implied in a sequential model for a Bi-Bi reaction, i.e., a reaction that involves two reactants, A and B, and two products, P and Q, that a ternary complex EAB must form before any catalysis can occur and products can be released. A sequential mechanism is characterized by the fact



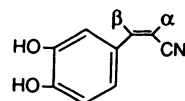
**Fig. 7.** Kinetics of inhibition of the EGFR-TK reaction by AG 537. The activity of EGFR was determined as described in the legend to Fig. 1, except that medium contained varying concentrations of GAT, 60 mM  $MgAc_2$ , 50 mM Tris-MES, pH 7.6, 1.5–2.5  $\mu Ci$  of  $[\gamma\text{-}^{32}P]ATP$ , a fixed concentration of ATP (250  $\mu M$ ), and the following concentrations of AG 537:  $\Delta$ , 0.00;  $\triangle$ , 0.10;  $\diamond$ , 0.20;  $\square$ , 0.40;  $\bullet$ , 0.80;  $\circ$ , 2.0  $\mu M$ . The experimental results were analyzed as described in Data Analysis. Families of double-reciprocal plots for fits to eq. 4 for nonexclusive or partial inhibition (A), eq. 6 for competitive inhibition (B), eq. 8 for noncompetitive (or mixed-competitive) inhibition (C), or eq. 10 for inhibition competitive with both substrates (D) are shown.



**Fig. 8.** Slope replots of the family of curves shown in Fig. 7, A ( $\circ$ ), B ( $\bullet$ ), C ( $\Delta$ ), and D ( $\square$ ).

that the lines in a family of double-reciprocal plots ( $1/v$  versus  $1/[A]$  or  $1/[B]$ ) intersect at a common point on or to the left of the ordinate and above, below, or on the abscissa. In a random mechanism, the free enzyme can bind either substrate to form a binary complex, EA or EB, and the ternary complex can then be formed by the addition of the second substrate (21, 25–27). The present kinetic experiments can readily be interpreted on the basis of such a model.

Many of the tyrophostins examined in the present work have the following general structure:





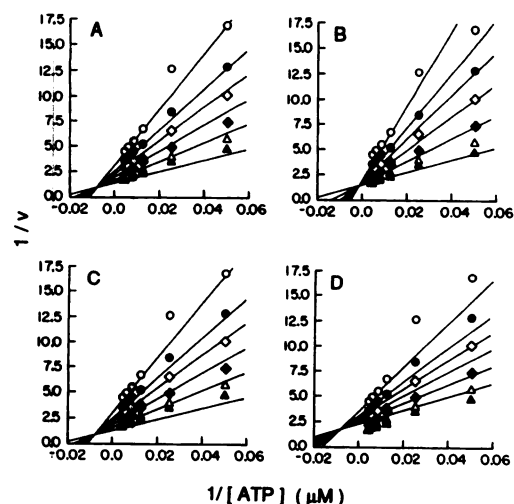


**Fig. 9.** Kinetics of inhibition of the EGFR-TK reaction by AG 538. The activity of EGFR was determined as described in the legend to Fig. 1 at the following concentrations of AG 538:  $\Delta$ , 0.0;  $\nabla$ , 0.1;  $\blacklozenge$ , 0.2;  $\diamond$ , 0.3;  $\bullet$ , 0.4;  $\circ$ , 0.6  $\mu\text{M}$ . The experimental results were analyzed as described in Data Analysis. Families of double-reciprocal plots for fits to eq. 3 for nonexclusive or partial inhibition (A), eq. 5 for competitive inhibition (B), eq. 7 for noncompetitive (or mixed-competitive) inhibition (C), or eq. 9 for inhibition competitive with both substrates (D) are shown.

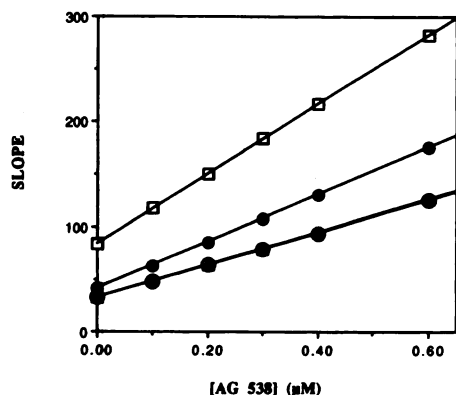


**Fig. 10.** Slope replots of the four families of double-reciprocal plots shown in Fig. 9, A ( $\circ$ ), B ( $\bullet$ ), C ( $\blacktriangle$ ), and D ( $\square$ ).

All compounds except AG 537 and AG 538 were found to act as competitive inhibitors with respect to both substrates of the EGFR kinase reaction. Because in the kinase reaction there is a direct transfer of phosphate from ATP to the tyrosine residue of the peptide substrate (9), both substrates of the kinase reaction must bind at the active center, in close proximity to one another. Because in all of the BMN tyrphostins examined there is a common structural element, i.e., the 3,4-dihydroxy-(*cis*)-cinnamitrile group, we propose that all of the BMN tyrphostins bind to the same site at the active center of the EGFR and thereby distort the latter to such an extent that in most cases neither substrate can bind to the receptor. In the case of AG 537 and AG 538, we suggest that the second dihydroxyphenyl group causes these tyrphostins to bind in such a way that they completely prevent the binding of GAT, whereas their effect on the binding of ATP is less pronounced ( $\gamma = 2.1$  in the case of AG 537 and 1.8 in the case of AG 538). Different possible modes of binding of the various tyrphostins at the EGFR-TK active center are displayed in Fig. 13. Fig. 13 illustrates that AG 538 can in principle bind in two similar

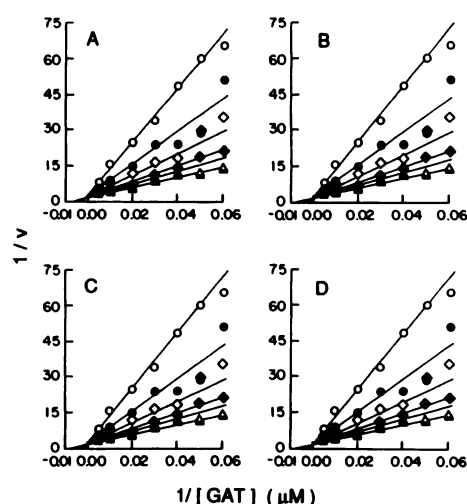


**Fig. 11.** Kinetics of inhibition of the EGFR-TK reaction by AG 538. The activity of EGFR was determined as described in the legend to Fig. 1, except that medium contained varying concentrations of GAT, 60 mM  $\text{MgAc}_2$ , 50 mM Tris-MES, pH 7.6, 1.5–2.5  $\mu\text{Ci}$  of [ $\gamma\text{-}^{32}\text{P}$ ]ATP, a fixed concentration of ATP (40  $\mu\text{M}$ ), and the following concentrations of AG 538:  $\Delta$ , 0.00;  $\nabla$ , 0.08;  $\blacklozenge$ , 0.15;  $\diamond$ , 0.30;  $\bullet$ , 0.60;  $\circ$ , 1.2  $\mu\text{M}$ . The experimental results were analyzed as described in Data Analysis. Families of double-reciprocal plots for fits to eq. 4 for nonexclusive or partial inhibition (A), eq. 6 for competitive inhibition (B), eq. 8 for noncompetitive (or mixed-competitive) inhibition (C), or eq. 10 for inhibition competitive with both substrates (D) are shown.

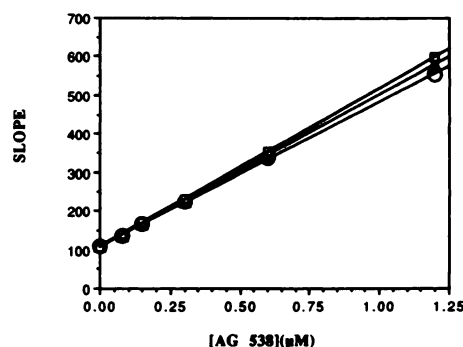


**Fig. 12.** Slope replots of the family of curves shown in Fig. 11, A ( $\circ$ ), B ( $\bullet$ ), C ( $\blacktriangle$ ), and D ( $\square$ ).

modes, one in which the main dihydroxybenzene ring binds at the tyrosine site and one in which the dihydroxyphenyl ring that is located in the  $\alpha$ -position binds at this site. Interestingly, AG 805 and AG 468, which possess only the dihydroxybenzene ring in the  $\alpha$ -position, affect both substrate binding sites and are thus competitive with both GAT and ATP, as indicated in Results. It seems, therefore, that the modes of binding of AG 805 and AG 468 are similar to that of AG 213 and other MBN tyrphostins and that AG 538 can actually bind as illustrated in Fig. 13. The R-groups in the  $\alpha$ -position of the various BMN tyrphostins determine their affinity for the receptor, i.e., their  $K_i$ .

The lavendustin derivatives with hydroxyl groups in positions 2 and 5 of the first phenyl ring and a carboxyl group *meta* to the NH group (AG 814) or *para* to the NH group (RG 14467) (28) are very potent EGFR-TK inhibitors. AG 814 has been found in the present studies to act as a pure competitive inhibitor with respect to both ATP and GAT. The lavendustin-like tyrphostin AG 826 is also a pure competitive inhibitor with respect to both GAT and ATP (Table 3). These two inhibitors

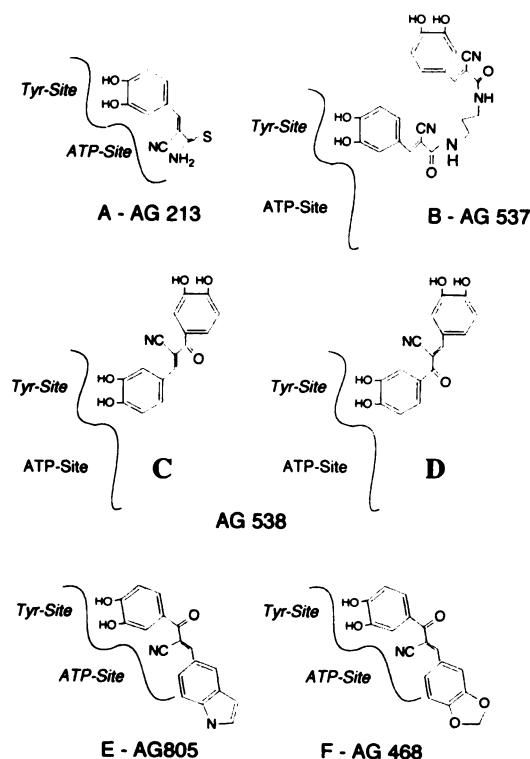


**Fig. 13.** Possible modes of interaction of various tyrphostins with the EGFR active center. A, BMN or 3,4-dihydroxy-(cis)-cinnamionitrile tyrphostins; B, AG 537; C and D, AG 538; E, AG 805; F, AG 468.

differ only with respect to the positions of the two hydroxyl groups of the first ring, i.e., 2,5-positions in AG 814 and 3,4-positions in AG 826, but they inhibit the EGFR-TK activity with  $K_i$  values that differ by almost 1 order of magnitude (Table 3). Erbstatin was reported previously to be a competitive inhibitor with respect to the peptide being phosphorylated and noncompetitive with respect to ATP (29) but was reported by Hsu et al. (30) to be a hyperbolic mixed-type inhibitor. In the present studies, however, this compound was found to be a competitive inhibitor with respect to both substrates. The differences between the cited studies and the data reported in the present work are most probably due to the procedures used for analyzing the experimental data. Because in our experiments we have used a more detailed and rigorous analytical procedure based on 42 experimental points, we feel confident that the results presented here are reliable. In view of the present findings, we suggest that the lavendustin derivatives and erbstatin bind and act by mechanisms similar to those proposed for the tyrphostins studied in the present work.

The present studies emphasize the usefulness of tyrphostins and our computer program as potent research tools. The kinetic models proposed for the action of tyrphostins on the EGFR-TK reaction should be most useful in the design of more specific and potent EGFR-TK inhibitors. The finding that AG 537 and AG 538 are competitive inhibitors with respect to the peptide substrate and noncompetitive with ATP is important for the design of future TK blockers. If one is to use PTK blockers in future therapies, preferred drugs will be those that are competitive only for the tyrosine substrate site, because such blockers could be selective for different TKs. A blocker that is competitive with respect to ATP is likely to be nondiscriminatory *in vivo* because of the high intracellular ATP concentrations, as

demonstrated by us recently for tyrphostins aimed at EGFR/HER-1 and HER-2/*neu* (15). As discussed above, all of the BMN tyrphostins examined contain the 3,4-dihydroxy-(cis)-cinnamionitrile group as a common structural element. These tyrphostins seem to bind to the same site at the active center of the EGFR. It is reasonable to assume that modifications at the primary ring of the BMN tyrphostins might direct this group and enable it to specifically bind to the ATP site. If such EGFR-TK inhibitors contained the second dihydroxyphenyl group of AG 537 or AG 538, or a modification of these groups, one would expect these tyrphostins to act as bi-substrate inhibitors that would simultaneously prevent the binding of both substrates to the receptor. Further attempts may be directed to increasing the affinities of such inhibitors for the receptor. In other words, the present studies lay the foundation for the development and evaluation of the mode of action of novel inhibitors that should be both highly selective and efficient at low concentrations.

#### References

- Ullrich, A., and J. Schlessinger. Signal transduction by receptors with tyrosine kinase activity. *Cell* 61:203-212 (1990).
- Carpenter, G., and S. Cohen. Epidermal growth factor. *J. Biol. Chem.* 265:7709-7712 (1990).
- Hanks, S. K., A. M. Quinn, and T. Hunter. The protein kinase family: conserved features and deduced phylogeny of the catalytic domains. *Science (Washington D. C.)* 241:45-52 (1988).
- Posner, I., M. Engel, and A. Levitzki. Kinetic model of the epidermal growth factor (EGF) receptor tyrosine kinase and a possible mechanism of its activation by EGF. *J. Biol. Chem.* 267:20638-20647 (1992).
- Yaish, P., A. Gazit, C. Gilon, and A. Levitzki. Blocking of EGF-dependent cell proliferation by EGF receptor kinase inhibitors. *Science (Washington D. C.)* 242:933-935 (1988).
- Gazit, A., P. Yaish, C. Gilon, and A. Levitzki. Tyrphostins. I. Synthesis and biological activity of protein tyrosine kinase inhibitors. *J. Med. Chem.* 32:2344-2352 (1989).
- Gazit, A., N. Osherov, I. Posner, P. Yaish, E. Poradosu, C. Gilon, and A. Levitzki. Tyrphostins. II. Heterocyclic and  $\alpha$ -substituted benzonemalononitrile tyrphostins as potent inhibitors of EGF receptor and *ErbB2/neu* tyrosine kinases. *J. Med. Chem.* 34:1897-1907 (1991).
- Levitzki, A. Tyrphostins: potential antiproliferative agents and novel molecular tools. *Biochem. Pharmacol.* 40:913-918 (1990).
- Levitzki, A. Tyrphostins: tyrosine kinase blockers as novel antiproliferative agents and dissectors of signal transduction. *FASEB J.* 6:3275-3282 (1992).
- Lyall, R. M., A. Zilverstein, A. Gazit, C. Gilon, A. Levitzki, and J. Schlessinger. Tyrphostins inhibit EGF receptor tyrosine kinase activity in living cells and EGF-stimulated cell proliferation. *J. Biol. Chem.* 264:14503-14509 (1989).
- Margolis, B., S. G. Rhee, S. Felder, R. Lyall, A. Levitzki, A. Ullrich, A. Zilverstein, and J. Schlessinger. EGF-induced tyrosine phosphorylation of phospholipase C-II: a potential mechanism for EGF-receptor signalling. *Cell* 57:1101-1107 (1989).
- Posner, I., A. Gazit, C. Gilon, and A. Levitzki. Tyrphostins inhibit the epidermal growth factor receptor-mediated breakdown of phosphoinositides. *FEBS Lett.* 257:287-291 (1989).
- Dvir, A., Y. Milner, O. Chomsky, C. Gilon, A. Gazit, and A. Levitzki. The inhibition of EGF-dependent proliferation of keratinocytes by tyrosine kinase blockers. *J. Cell Biol.* 113:857-865 (1991).
- Anafi, M., A. Gazit, C. Gilo, Y. Ben-Neriah, and A. Levitzki. Selective interactions of transformed and normal *abl* proteins with ATP, tyrosine-copolymer substrates and tyrphostins. *J. Biol. Chem.* 267:4518-4523 (1992).
- Osherov, N., A. Gazit, C. Gilon, and A. Levitzki. Selective inhibition of the epidermal growth factor and *Her2/neu* receptor by tyrphostins. *J. Biol. Chem.* 268:11134-11142 (1993).
- Umezawa, H., M. Imoto, T. Sawa, K. Ishiki, N. Matsuda, M. Uchida, H. Iinuma, M. Hamada, and T. Takeuchi. Studies on a new EGF receptor kinase inhibitor, erbstatin, produced by MH 435-RF3. *J. Antibiot. (Tokyo)* 39:170-173 (1986).
- Onoda, T., H. Inuma, Y. Sasaki, M. Hamada, K. Ishihara, H. Naganawa, T. Takeuchi, K. Tatsuta, and K. Umezawa. Isolation of a novel tyrosine kinase inhibitor, lavendustin-A from *Streptomyces griseolavendus*. *J. Nat. Prod. (Lloydia)* 52:1252-1257 (1989).
- Sinhababu, A. K., and R. T. Borchardt. Selective ring C-methylation of hydroxybenzaldehydes via their Mannich bases. *Synth. Commun.* 13:677-681 (1983).
- Yarden, Y., and J. Schlessinger. Self-phosphorylation of epidermal growth factor receptor: evidence for a model of intermolecular allosteric activation. *Biochemistry* 26:1434-1442 (1987).

20. Levitzki, A., A. Gazit, N. Osherov, I. Posner, and C. Gilon. Inhibition of protein tyrosine kinases by tyrphostins. *Methods Enzymol.* **207**:347-361 (1991).
- 20a. *IMSL MATH/LIBRARY for Mathematical Applications, Version 2.0 User's Manual*. Houston, 965-1134 (1991).
21. Segel, I. M. *Enzyme Kinetics*. Wiley, New York, 273-337 (1975).
22. Cleland, W. W. Kinetics of enzyme-catalyzed reactions with two or more substrates or products. 1. Nomenclature and rate equations. *Biochim. Biophys. Acta* **67**:104-137 (1963).
23. Posner, I., C.-S. Wang, and W. J. McConathy. The comparative kinetics of soluble and heparin-Sepharose immobilized lipoprotein lipase. *Arch. Biochem. Biophys.* **226**:306-316 (1983).
24. Cleland, W. W. Statistical analysis of enzyme kinetic data. *Methods Enzymol.* **63**:108-138 (1979).
25. Fromm, H. J. Summary of kinetic reaction mechanisms. *Methods Enzymol.* **63**:42-53 (1979).
26. Fromm, H. J. Use of competitive inhibitors to study substrate binding order. *Methods Enzymol.* **63**:467-483 (1979).
27. Rudolph, F. B. Product inhibition and active complex formation. *Methods Enzymol.* **63**:411-436 (1979).
28. Hsu, C.-Y., P. E. Persons, A. P. Spada, R. A. Bendor, A. Levitzki, and A. Zilberstein. Kinetic analysis of the inhibition of the EGF receptor tyrosine kinase by lavendustin-A and its analogue. *J. Biol. Chem.* **266**:21105-21112 (1991).
29. Imoto, M., K. Umezawa, K. Isshiki, S. Kunimoto, T. Sawa, T. Takeuchi, and H. Umezawa. Kinetic studies of tyrosine kinase inhibitors by erbetatin. *J. Antibiot. (Tokyo)* **4**:1471-1473 (1987).
30. Hsu, C.-Y., M. V. Jakoski, M. P. Maguire, A. P. Spada, and A. Zilberstein. Inhibition kinetics and selectivity of the tyrosine kinase inhibitor erbetatin and a pyridone-based analog. *Biochem. Pharmacol.* **43**:2471-2477 (1992).

---

Send reprint requests to: Alexander Levitzki, Department of Biological Chemistry, Institute of Life Sciences, The Hebrew University of Jerusalem, Jerusalem, 91904, Israel.

---